Molecular Crystals and Liquid Crystals Science and Technology. Section A. Molecular Crystals and Liquid Crystals

Publication details, including instructions for authors and subscription information:
http://www.tandfonline.com/loi/gmcl19

Molecular Field Theory of The Frederiks Transition and its Monte Carlo Confirmation

Y. Yang [a], J. Lu [a], H. Zhang [a] & D. Yan [a]

[a] Department of Macromolecular Science, Fudan University, Shanghai, 200433, People's Republic of China

Version of record first published: 23 Sep 2006.

To cite this article: Y. Yang , J. Lu , H. Zhang & D. Yan (1995): Molecular Field Theory of The Frederiks Transition and its Monte Carlo Confirmation, Molecular Crystals and Liquid Crystals Science and Technology. Section A. Molecular Crystals and Liquid Crystals, 259:1, 23-36

To link to this article: http://dx.doi.org/10.1080/10587259508038670

Mol. Cryst. Liq. Cryst., 1995, Vol. 259, pp. 23–36
Reprints available directly from the publisher
Photocopying permitted by license only

Molecular Field Theory of The Frederiks Transition and its Monte Carlo Confirmation

Y. YANG*, J. LU, H. ZHANG, and D. YAN

Department of Macromolecular Science, Fudan University, Shanghai 200433, People's Republic of China

(Received June 10, 1994; in final form June 10, 1994)

The molecular field theory of the Frederiks transition has been developed based on the Lebwohl-Lasher nematogen model and localized mean field approximation. We found that it needs five order parameters to generally describe the nematic system with boundaries. For the splay type of cell configuration, two of these order parameters are zeros. The theoretically calculated results are further confirmed by corresponding Monte Carlo simulation using Lebwohl-Lasher nematogen model as the prototype of the liquid crystal and the agreement is quite good considering the simplicity of the theory. The experimental law and the predictions of classical anisotropic continuum media theory are also reproduced by the present molecular field theory. Therefore, the results obtained in this paper lend a support to the general validity of the Lebwohl-Lasher nematogen model for the theoretical studies of small molecular liquid crystals.

Keywords: Liquid crystals, Frederiks transition, Lebwohl-Lasher model, Monte Carlo simulation, molecular field theory

1. INTRODUCTION

A consequence of the anisotropy of the diamagnetic and dielectric susceptibilities is that an ensemble of nematic liquid crystal molecules in an external magnetic or electric field has a well defined orientational configuration of the molecular axes (or directors) relative to the field which is corresponding to the minimum of the free energy. With positive values of $\Delta\chi$ and $\Delta\varepsilon$, the anisotropy of diamagnetic and electric susceptibilities, the director tends to align itself along the field direction; with negative values, a perpendicular alignment is induced. This effect was discovered and studied in detail by Frederiks *et al.*[1] over sixty years ago. Soon after, Zocher set up a first version of the continuum theory.[21] A more complicated theory of Frederiks transition, in which the Frank's elastic constants are regarded as being different, is given by Deuling[28] and Gruler *et al.*[29] It has been shown that the usual Frederiks transitions in insulating nematic liquid crystals are always second order.[14] Deuling *et al.*[24] proposed that if the conductive anisotropy in a conducting nematic liquid crystal is large enough, the deformation of the molecules can exhibit a discontinuous change and hysteresis. Lately the optically induced and enhanced first-order Frederiks transition in nematics has

* To whom the correspondence should be addressed.

received particular attention. The theoretical prediction of this kind of first-order transition was provided by Ong.[25] In addition, the magnetic-field and electric field induced by first-order optical Frederiks transition in a nematic film was observed experimentally.[26, 27] Due to its importance for liquid crystalline displays, the computation of its director configuration under various external field has been a matter of continued interest. However, in most calculations, the director configuration is calculated by numerical integration of a set of differential equations obtained by applying the Euler-Lagrange equations on the Frnak's free energy,[2–4] or by using simulated-anneal technique to search the minimum[5] of the Frank's free energy. However, to our knowledge, the molecular field theory of the Frederiks transition has not yet been worked out. Therefore, it is the main motivation of this work to understand the Frederiks transition on the level of molecular field theory.

Figure 1 represents the three basic cell configurations in the study of the Frederiks transition, which correspond to the splay (S), bend (B), and twist (T) deformations in nematic liquid crystals. In this paper, we first present a very simple mean field molecular theory for describing the usual Frederiks transition based on the Lebwohl-Lasher nematogenic model.[6,7] Advantages of the Lebwohl-Lasher molecular model are that it can take the temperature dependence of the Frederiks transition into account and the model can be considered as the prototype for computer simulations[8–10,16] and theoretical calculations[11–13] for the nematic system. Therefore, the mean field theoretical predictions then are confirmed further by Monte Carlo simulation in this work. The comparison between molecular theory presented in this paper and the classical anisotropic continuum media theory[14] is also made.

The paper is organized as follows. In section II, five order parameters are introduced to describe the nematic director configurations in an unsymmetrical nematic liquid crystalline system. Then the mean field molecular theory for the Frederiks transition is formulated based on the Lebwohl-Lasher nematic model. In section III, the Monte Carlo simulation algorithm based on the same model is described. The results and the comparison between the mean field calculations and Monte Carlo simulations are presented in section IV. Finally, the brief summary and the conclusions are given in section V.

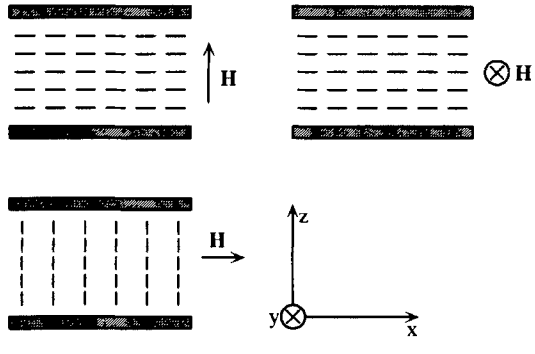

FIGURE 1 Schematic drawing of the cell configurations for splay (S), twist (T) and bend (B) deformations.

2. MEAN FIELD THEORY

2.1. The Model Potential

In the Lebwohl-Lasher model,[6,7] a system of uniaxial particles placed at the sites of a cubic lattice interacting with a purely second rank pair potential,

$$U_{i,j} = -\varepsilon_{ij} P_2(\cos\theta_{ij}) \tag{1}$$

here $\varepsilon_{ij} = \varepsilon_b$, a positive constant, is a parameter representing the strength of the attractive interaction for molecules i and j being nearest neighbors; $P_2(\cos\theta_{ij})$ is a second order Legendre polynomial with $\cos\theta_{ij}$ measuring the angle between the symmetry axes of two molecules. From a formal point of view, Eq. (1) is a simplified version of the attractive anisotropic interaction put forward by Maier and Saupe.[15] Therefore, Lebwohl-Lasher model can be considered as the descretized version of Maier-Saupe model.

For later convenience, $P_2(\cos\theta_{ij})$ can be expanded as,

$$\begin{aligned} P_2(\cos\theta_{ij}) &= P_2(\cos\theta_i) P_2(\cos\theta_j) + 2\sum_{k=1}^{2} \frac{(2-k)!}{(2+k)!} P_2^k(\cos\theta_i) P_2^k(\cos\theta_j) \cos[k(\phi_i - \phi_j)] \\ &= P_2(\cos\theta_i) P_2(\cos\theta_j) + 3\sin\theta_i \cos\theta_i \cos\phi_i (\sin\theta_j \cos\theta_j \cos\phi_j) \\ &\quad + 3\sin\theta_i \cos\theta_i \sin\phi_i (\sin\theta_j \cos\theta_j \sin\phi_j) + \tfrac{3}{4}\sin^2\theta_i \cos 2\phi_i (\sin^2\theta_j \cos 2\phi_j) \\ &\quad + \tfrac{3}{4}\sin^2\theta_i \sin 2\phi_i (\sin^2\theta_j \sin 2\phi_j) \end{aligned} \tag{2}$$

where θ_i and ϕ_i are the polar angles between the symmetry axis of i-th nematogen and the z direction of lab frame (or the local director for bulk nematic system). If the molecule i is selected as a probe, the local mean field potential of molecule i can be obtained by averaging the orientation of its nearest neighbor j, i.e.,

$$\begin{aligned} U_i = -\varepsilon_b [&P_2(\cos\theta_i) \cdot \bar{P}_{2j} + 3\sin\theta_i \cos\theta_i \cos\phi_i \cdot \sigma_j + 3\sin\theta_i \cos\theta_i \sin\phi_i \cdot \sigma'_j \\ &+ \tfrac{3}{4}\sin^2\theta_i \cos 2\phi_i \cdot \delta_j + \tfrac{3}{4}\sin^2\theta_i \sin 2\phi_i \cdot \delta'_j] \end{aligned} \tag{3}$$

where $\bar{P}_2$, σ, σ', δ and δ' are the order parameters of the molecule j, which are defined as follows,

$$\bar{P}_{2j} = \langle \tfrac{1}{2}(3\cos^2\theta_j - 1) \rangle \tag{4}$$

$$\sigma_j = \langle \sin\theta_j \cos\theta_j \cos\phi_j \rangle \tag{5}$$

$$\sigma'_j = \langle \sin\theta_j \cos\theta_j \sin\phi_j \rangle \tag{6}$$

$$\delta_j = \langle \sin^2\theta_j \cos 2\phi_j \rangle \tag{7}$$

$$\delta'_j = \langle \sin^2\theta_j \sin 2\phi_j \rangle \tag{8}$$

where the angular brackets denote an ensemble average over the orientation of the nematogen. The model potential given in Eq. (3) together with Eqs. (4)–(8) is quite universal, it is suitable for the system with any kind of cell symmetry. Obviously, we have nonzero $\bar{P}_2$ but zero σ, σ', δ and δ' for a normal bulk system due to the uniformly distributed ϕ_j. For the S type deformation, which we will discuss in detail, the cell configuration is symmetry about x axis due to the existence of oriented surface anchoring, i.e., the nematogen with the orientation (θ, ϕ) and $(\theta, -\phi)$ feels the same field. This results in the order parameters σ' and δ' being zeros. Therefore, the modeled mean field potential for the S type cell configuration can be simplified to,

$$U_i = -\varepsilon_b[P_2(\cos\theta_i)\cdot\bar{P}_{2j} + 3\sin\theta_i\cos\theta_i\cos\phi_i\cdot\sigma_j + \tfrac{3}{4}\sin^2\theta_i\cos 2\phi_i\cdot\delta_j] \tag{9}$$

The external field for the S type cell configuration is assumed to be along the z direction, see Figure 1. The external field (magnetic field) exerts an extra potential on molecule i, which can be written as,

$$U_{hi} = -\tfrac{1}{2}\Delta\chi(n_i\cdot\mathrm{H})^2 = -\tfrac{1}{2}\Delta\chi\mathrm{H}^2\cos\theta_i = -\varepsilon_h\cos^2\theta_i \tag{10}$$

where $\Delta\chi$ is the anisotropy of the magnetic susceptibility, and H is the strength of the magnetic field. Therefore, the total model potential for the S type Frederiks transition is simply the sum of Eqs. (9–10).

In the following discussion, we will restrict ourselves mainly to the S type cell configuration. However, the extension to the cases of B and T cell configurations is straight forward, and needs no detailed explanation.

2.2. Mean field Theory of the Frederiks Transition

The molecular theory for the Lebwohl-Lasher model in the surface anchored state has been given previously[13] and so we simply sketch the principle results. Considering an S type cell, it has two substrates in the xy plans located at the positions $z = 0$ and $d + 1$ as shown in Figure 2. The surface orientational field of the substrates is assumed to be along x axis. The cell with thickness d is divided into a cubic lattice with d layers along z direction and we label the layers parallel to the substrates with the letter m, where m equals 1 and d denotes two interfacial layers. The transitional symmetry along x and y axes is assumed. Although this symmetry will be broken when the domain wall structure is existed, this assumption is held for the uniformly anchored system. For the cubic lattice, the coordination number $z = 6$ with 4 nearest neighbors are in the same layer and another two are in the upper layer and down layer, respectively. Therefore, the potential of molecules in the m-th layer $(1 < m < d)$ can readily be written as,

$$\begin{aligned} U_m = &-\varepsilon_b(\bar{P}_{2,m-1} + 4\bar{P}_{2,m} + \bar{P}_{2,m+1})P_2(\cos\theta_m) \\ &- 3\varepsilon_b\sin\theta_m\cos\theta_m\cos\phi_m(\sigma_{m-1} + 4\sigma_m + \sigma_{m+1}) \\ &- \tfrac{3}{4}\sin^2\theta_m\cos 2\phi_m(\delta_{m-1} + 4\delta_m + \delta_{m+1}) - \varepsilon_h\cos^2\theta_m \end{aligned} \tag{11}$$

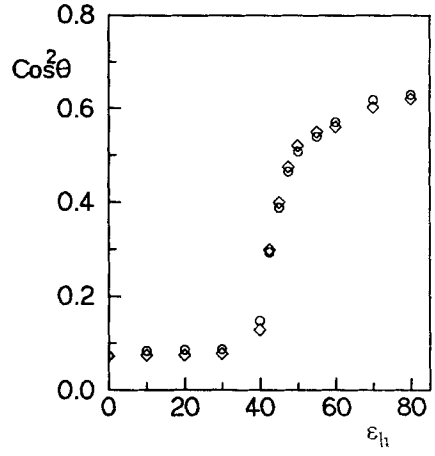

FIGURE 2 Monte Carlo simulated results of $\langle\cos^2\theta\rangle$ vs. ε_h for the Frederiks transition of S and B cell configurations. The parameters are: $d = 11$. $\varepsilon_s/\varepsilon_b = 1$, $T^* = kT/\varepsilon_b = 0.741$, $\diamond$: **B** deformation; O: S deformation. It indicates that the Frank's elastic constants k_{11} and k_{33} are equal for the Lebwohl-Lasher model potential.

For the surface anchored layers ($m = 1$ and d), we have

$$U_1 = -\varepsilon_b[(4\bar{P}_{2,1} + \bar{P}_{2,2})P_2(\cos\theta_1) + 3(4\sigma_1 + \sigma_2)\sin\theta_1\cos\theta_1\cos\phi_1 + \tfrac{3}{4}(4\delta_1 + \delta_2)\sin^2\theta_1\cos 2\phi_1] - \varepsilon_s P_2(\sin\theta_1\cos\phi_1) - \varepsilon_h\cos^2\theta_1 \tag{12}$$

and

$$U_d = -\varepsilon_b[(4\bar{P}_{2,d} + \bar{P}_{2,d-1})P_2(\cos\theta_d) + 3(4\sigma_d + \sigma_{d-1})\sin\theta_d\cos\theta_d\cos\phi_d + \tfrac{3}{4}(4\delta_d + \delta_{d-1})\sin^2\theta_d\cos 2\phi_d] - \varepsilon_s P_2(\sin\theta_d\cos\phi_d) - \varepsilon_h\cos^2\theta_d \tag{13}$$

where ε_s is the strength of the surface anchoring. Equations (10)–(13) are only suitable for the S type cell configuration, the extension to the other cell configurations is straight forward. From Eqs. (11)–(13), the partition function for m-th layer is simply written as

$$Z_m = \int_0^{\pi}\int_0^{2\pi} \exp\left(-\frac{U_m}{KT}\right)\sin\theta_m d\theta_m d\phi_m \tag{14}$$

and the Helmholtz free energy of nematogens in cell of S type configuration is obtained by summing over the contributions from each layer,

$$\frac{F}{n^2} = \frac{\varepsilon_b}{2}\left[(4\bar{P}_{2,1} + \bar{P}_{2,2})\bar{P}_{2,1} + 3(4\sigma_1 + \sigma_2)\sigma_1 + \frac{3}{4}(4\delta_1 + \delta_2)\delta_1\right] + \frac{\varepsilon_s}{2}\left(\frac{9\sigma_1^2}{2\bar{P}_{2,1} + 1} - 1\right)$$

$$+ \sum_{m=1}^{d-1}\frac{\varepsilon_b}{2}\Big[(\bar{P}_{2,m-1} + 4\bar{P}_{2,m} + \bar{P}_{2,m+1})\bar{P}_{2,m} + 3(\sigma_{m-1} + 4\sigma_m + \sigma_{m+1})\sigma_m$$

$$+\frac{3}{4}(\delta_{m-1}+4\delta_m+\delta_{m+1})\delta_m\Big]+\frac{\varepsilon_b}{2}\Big[(4\bar{P}_{2,d}+\bar{P}_{2,d-1})\bar{P}_{2,d}+3(4\sigma_d+\sigma_{d-1})\sigma_d$$

$$+\frac{3}{4}(4\delta_d+\delta_{d-1})\delta_d\Big]+\frac{\varepsilon_s}{2}\left(\frac{9\sigma_d^2}{2\bar{P}_{2,d}+1}-1\right)+\sum_{m=1}^{d}\left[\varepsilon_h\frac{2\bar{P}_{2,m+1}}{3}-kT\ln Z_m\right] \quad (15)$$

where n^2 is the number of nematogens in each layer. The order parameters can be obtained by solving the following coupled self-consistency equations,

$$\bar{P}_{2,m}=Z_m^{-1}\int_0^{\pi}\int_0^{2\pi}P_2(\cos\theta_m)\exp\left(-\frac{U_m}{kT}\right)\sin\theta_m d\theta_m d\phi_m \quad (16)$$

$$\sigma_m=Z_m^{-1}\int_0^{\pi}\int_0^{2\pi}\sin\theta_m\cos\theta_m\cos\phi_m\exp\left(-\frac{U_m}{kT}\right)\sin\theta_m d\theta_m d\phi_m \quad (17)$$

$$\delta_m=Z_m^{-1}\int_0^{\pi}\int_0^{2\pi}\sin^2\theta_m\cos 2\phi_m\exp\left(-\frac{U_m}{kT}\right)\sin\theta_m d\theta_m d\phi_m \quad (18)$$

which minimize the free energy of Eq. (15). The iteration procedure can be summarized as follows: Provisional values of $\bar{P}_{2,m}$, σ_m and δ_m serve as the numerical evaluation of the partition functions (Eq. (14)) which subsequently yield improved $\bar{P}_{2,m}$, σ_m and δ_m via Eqs. (16) to (18). The calculation goes through each layer and the iteration is repeated until self-consistency is achieved. Trial calculations demonstrate that this iteration procedure does minimize the Helmholtz free energy of Eq. (15).

3. THE MONTE CARLO SIMULATION

The theory given in Sec. II is subjected to the mean field approximation. In this section we use the Lebwohl-Lasher model nematogen as the prototype of the Monte Carlo simulation, which is free of the mean field approximation, to confirm the general validity of the mean field approximation used in our theory.

The Monte Carlo simulations reported in this paper were performed on a $10 \times 10 \times d$ cubic lattice with periodic boundary conditions in x and y directions. The particles are assumed to interact through the nearest neighbor Lebwohl-Lasher potential given in Eq. (1) except the interfacial layers of $m = 1$ and d. The substrates exert an orientational potential along the x direction with the maximal energy ε_s for S type cell configuration. The other cell configurations can be achieved simply by changing the orientational field direction of the substrates. The simulation procedure is quite similar to what has been commonly used in the literature[6,8-10] and in our previous publications.[13,16,17] In the Monte Carlo algorithm the orientation of the nematogen is described by its directional cosines and determined by a random unit vector that is uniformly distributed on the surface of a unit sphere. The orientation of each particle was changed using the procedure proposed by Barker and Watts.[18] The

simulation was performed for a series of increasing external field ε_h; the starting configuration for the lowest ε_h was perfectly oriented along the x direction. The system was equilibrated for about 5000 Monte Carlo cycles and thus rejected when calculating averages, where one Monte Carlo cycle represents $10 \times 10 \times d$ attempted moves. The production runs also consisted of approximately 5000 cycles, although this was divided into ten equal macrocycles and averages were obtained for each macrocycles to estimate the statistical errors. For the ε_h value close to the Frederiks transition, 10^4 Monte Carlo cycles have been used for the averages.

The simulated order parameters are obtained according to the definitions given in Eqs. (4–8). For the S type cell configuration, the simulations demonstrate that both σ'_m and δ'_m are zeros due to the symmetry of the cell configuration.

We should mention, before the detailed discussion, that the Frank's elastic constants k_{11}, k_{22} and k_{33} are equal for the present model due to the simplicity of the model potential. Figure 2 illustrates the typical results for the Frederiks transitions of S and B types of deformation. Certainly, the system with unequal Frank's elastic constants can also be simulated with modified potential.[19] This is beyond the main objective of the present work but opens the possibility for the future publications.

4. RESULTS AND DISCUSSIONS

4.1. Comparison between Mean field Theory and Monte Carlo Simulation

Both mean field molecular theory and Monte Carlo results revealed that the Frederiks transition is second-order. However, due to neglect of the fluctuation in the mean field treatment, the Lebwohl-Lasher model gives a reduced nematic-isotropic transition temperature for the bulk system, $T_{NI}^{(MF)*} = kT_{NI}/\varepsilon_b = 1.321$,[12] which is higher than the Monte Carlo simulated result, $T_{NI}^{(MC)*} = 1.116 \pm 0.005$.[12,16] Therefore, Luckhurst[12] suggested that the scaled dimensionless temperatures, T/T_{NI}, should be used for the comparison between the mean field calculation and Monte Carlo data or experimental data. This suggestion has been followed in this paper. For the same reason, the critical external field strength, ε_h^c, for the Frederiks transition should also be dealt with in the same way. For the case of $\varepsilon_s/\varepsilon_b = 1$, $d = 11$ and $T/T_{NI} = 0.9241$, the mean field calculation gives the reduced critical external field, $\varepsilon_h^c/\varepsilon_b = 0.072$, while the Monte Carlo results give $\varepsilon_h^{c(MC)}/\varepsilon_b = 0.085 \pm 0.005$ for the system $10 \times 10 \times 11$, where $\varepsilon_h^{c(MC)}$ is obtained from the $\bar{P}_2 \sim \varepsilon_h$ curve averaged over the layers. The simulation has also been performed on a lattice of $21 \times 21 \times d$ and $\varepsilon_h^{c(MC)}/\varepsilon_b = 0.090 \pm 0.005$ has been obtained. However, due to the fact that our system is confined in two substrates which is the natural boundary condition of our system, the usual finite-size scaling law[28] can't be applied to scale our Monte Carlo data for different sizes of x and y directions. Therefore, in the following discussion, we focus our attention on the system of $10 \times 10 \times d$. Although the data are not obtained by exploring to the limit of $L \to \infty$, the qualitative conclusions should not be altered. The comparison between Monte Carlo data and mean field theory indicated that the fluctuation, which is neglected in the mean field theory, not only drives the system more disorder, but also resists the external field. Therefore, the scaled dimensionless external field strength $\varepsilon_h/\varepsilon_h^c$ is used

for the comparison between theory and Monte Carlo simulation as suggested by Luckhurst.[12]

Figure 3 presents the comparison of external field strength dependencies of the order parameters $\bar{P}_2$, σ and δ obtained by theory and Monte Carlo simulation. The agreement is fairly good considering the simplicity of the present theoretical model. It can be clearly seen that the interfacial layers, $m = 1$ and d, are hardly deformed due to the relatively strong surface anchoring. All the other layers ($m = 2$ to d-1) clearly show the threshold values of ε_h^c, e.g., the order parameters do not change too much until ε_h^c has been reached. An interesting characteristic is that the value of σ has a maxima for the layers close to the middle of the cell near the threshold field strength. To see the relations among three order parameters more clearly, Figure 4 shows the external field strength dependencies of the order parameters for the middle layer ($m = 6$). From the geometric connotation of these order parameters, $\bar{P}_2$ can be thought of the z-projection

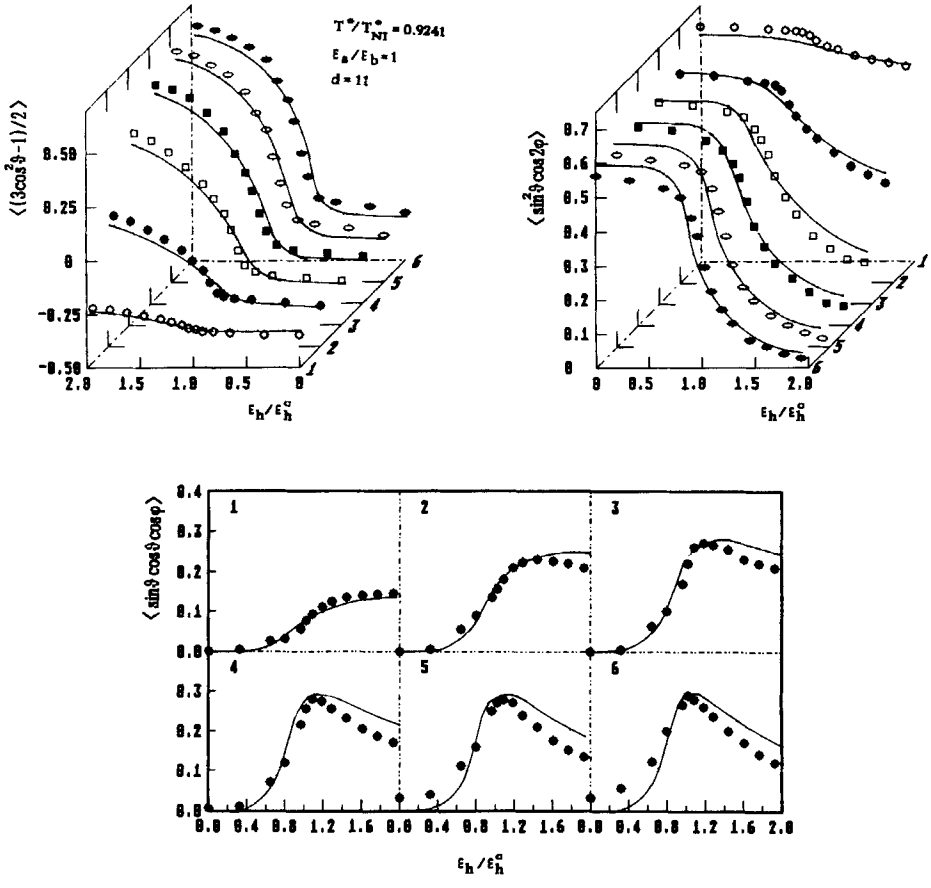

FIGURE 3 The comparison between the Monte Carlo simulation and the meanfield theoretical calculation on the order parameters P_2, δ and σ. The parameters are: $d = 11$, $T/T_{NI} = 0.9241$, $\varepsilon_s/\varepsilon_b = 1$. The symbols are the Monte Carlo data and the solid lines are the results of meanfield calculation. The integer numbers in the figures are the layer numbers, m.

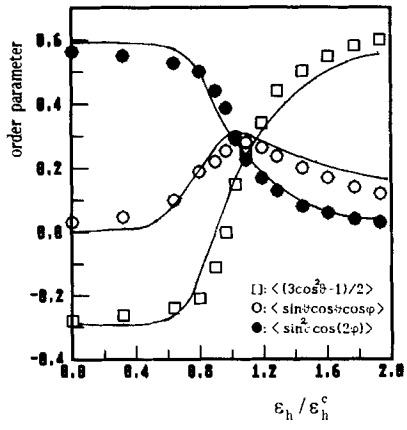

FIGURE 4 The order parameters for the middle layer ($m = 6$). The symbols are the Monte Carlo data and the solid lines are the results of meanfield calculation. The parameters of the simulation are the same as that of Figure 3.

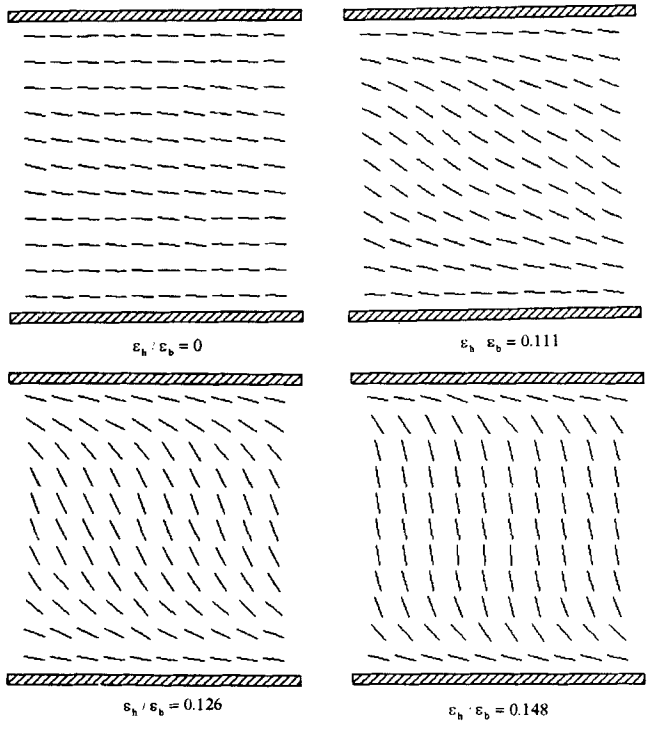

FIGURE 5 The snapshot pictures of the director configurations under different strength of external field. To give two dimensional representation, the orientation of each nematogen in the figure has been averaged over the lattices along the y direction. The simulation parameters are the same as that of Figure 3.

of the rod axis, δ reflects the x-projection of rod axis, while σ relates to the product of x and y components of the rod axis. As the external field strength increases, therefore, $\bar{P}_2$ increases due to the fact that the molecules tend to align along the z-direction (field direction). However, δ decreases with increasing external field strength which overcomes the x-direction anchoring. Thus $\bar{P}_2$ and δ will approach their limiting values of 1 and 0 for very high field strength. The order parameter σ, which is the compromise of $\bar{P}_2$ and δ, reaches the maxima when the x and y components of the rod axis are comparable. Although this interpretation is not as sophisticated, it provides an easy understanding of Frederiks transition. Figure 5 shows the snapshot pictures of Monte Carlo simulation which are quite helpful for better comprehension. In Figure 5, the orientation of each lattice in two-dimension representation has been averaged over the lattices along the y direction due to the translational symmetry of this direction.

To see the layer-dependence of the order parameters more clearly, Figure 6 shows the order parameters $\bar{P}_2$, δ and σ of different layers for three typical field strengths. The agreement between theory and Monte Carlo simulation is quite good. It is not

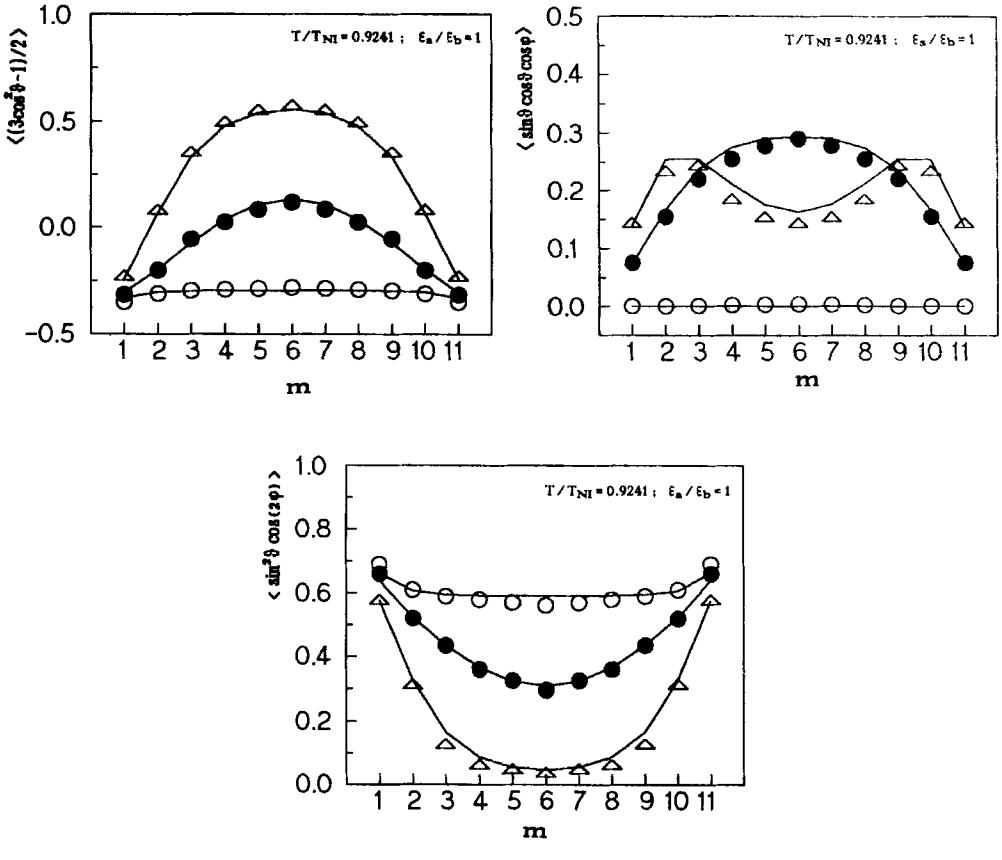

FIGURE 6 The layer dependence of the order parameters $\bar{P}_2$, (**a**); δ, (**b**) and σ, (**c**). The solid lines are the results of meanfield calculation and the symbols are the Monte Carlo data. O: $\varepsilon_h/\varepsilon_h^c = 0$; ●: $\varepsilon_h/\varepsilon_h^c = 1$; Δ: $\varepsilon_h/\varepsilon_h^c = 2$.

surprising that the deformation is started from the middle of the cell and then extended toward two substrates due to the relatively strong surface anchoring potential, $\varepsilon_s/\varepsilon_b = 1$.

Frederiks[20] showed experimentally that the critical field H_c was inversely proportional to the thickness d, i.e.,

$$H_c \cdot d = \text{const.} \tag{19}$$

Soon after, Zocher[21] set up a first version of the continuum theory and showed that Equation (19) is a natural consequence of it. Figure 7 shows the results of mean field calculation and Monte Carlo simulation. The Monte Carlo data shown in Figure 7 have been corrected by multiplying a factor of 0.072/0.085 due to the reason we mentioned at the beginning of this section. As is obvious from Figure 7, the Frederiks law, Equation (19), and the prediction of continuum theory[21] has been reproduced fairly both by the mean field molecular theory and the Monte Carlo simulation.

3.2. Temperature Dependence of the Frederiks Transition

Besides agreement between the molecular field theory developed here and the continuum theory, another advantage of the molecular theory is that the temperature dependence of the Frederiks transition can be easily taken into consideration. Figure 8 gives the molecular field theory calculated temperature dependence of the order parameters. As is clear from Figure 8, the threshold value of S type deformation considered here increases with decreasing temperature. Following the continuum theory, the critical field can be described by,

$$H_c = \pi \left(\frac{k_{11}}{\Delta\chi} \right)^{1/2} \frac{1}{d} \tag{20}$$

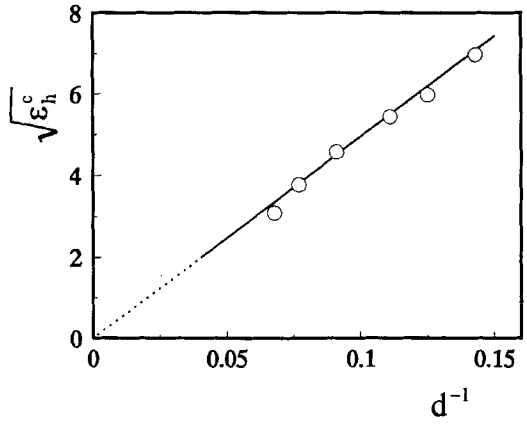

FIGURE 7 The plot of ε_h^c vs. d^{-1}. The solid line is the result of meanfield calculation and the symbols are the results of Monte Carlo simulation. The Monte Carlo data have been multiplied by a factor of 0.072/0.085. (see the main text for the details)

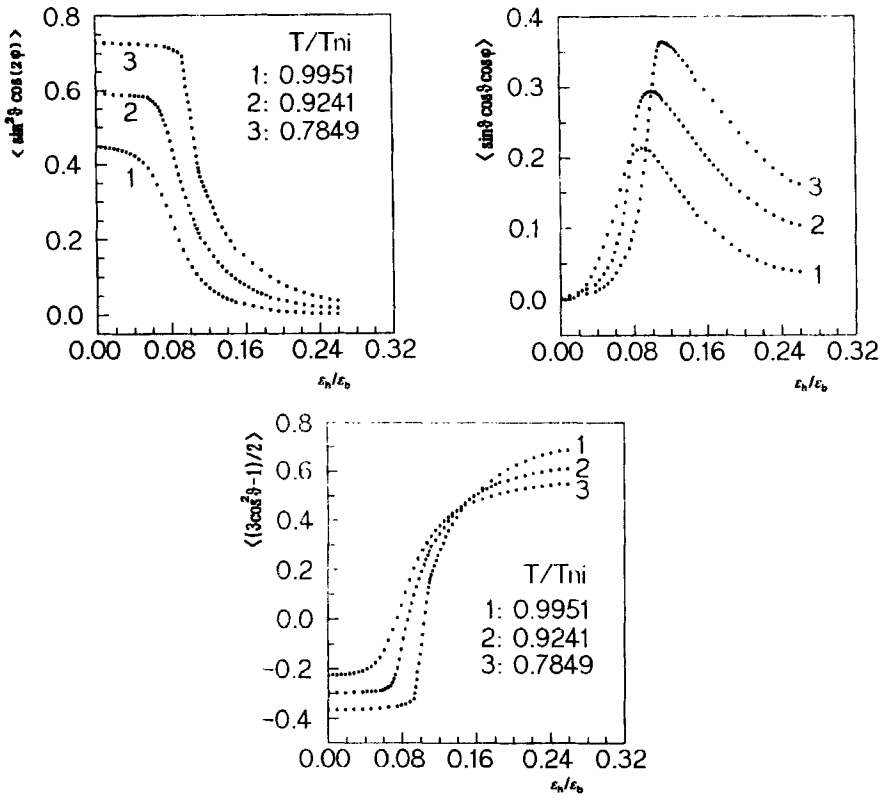

FIGURE 8 The meanfield calculation of temperature dependence of the Frederiks transition. The parameters used in the calculations are given in the insertion of Figure 8 (a).

On the other hand, the Frank's elastic constants have been proved to be proportional to the square of the orientational order parameter $(\bar{P}_2)_{\text{bulk}}$ in the bulk state.[22,23] Therefore, we expect that

$$H_c \propto (\bar{P}_2)_{\text{bulk}}, \quad \text{or,} \quad \sqrt{\frac{\varepsilon_h}{\varepsilon_b}} \propto (\bar{P}_2)_{\text{bulk}} \tag{21}$$

Equation (21) has been demonstrated both by molecular field theory and Monte Carlo simulation based on the Lebwohl-Lasher model, Figure 9. Thus, the Frederiks transition is related to the temperature through the orientational order parameter $(\bar{P}_2)_{\text{bulk}}$. The higher temperature results in lower order parameter $(\bar{P}_2)_{\text{bulk}}$, which corresponds to the lower Frank's elastic constant. Therefore, it needs lower external field to deform the nematogenic system for high temperature.

The similar results can also be obtained for B and T type cell configurations. The detailed discussions on B and T type deformations are beyond the main objective of this paper.

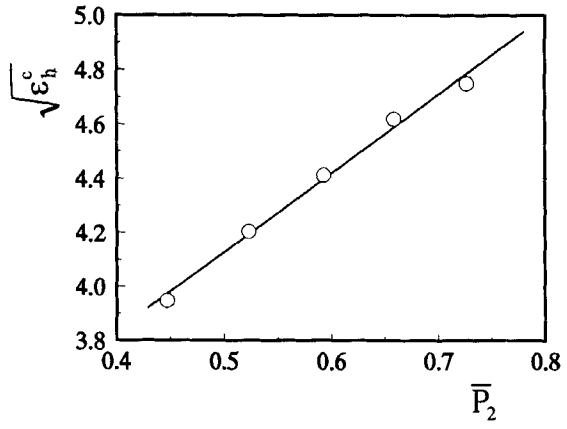

FIGURE 9 Critical field strength versus the order parameter in bulk state $(\bar{P}_2)_{bulk}$. The solid lines are the Monte Carlo data which are multiplied by a factor of 0.072/0.085. The calculation parameters are: $\varepsilon_s/\varepsilon_b = 1$, $d = 11$.

5. CONCLUSIONS

The molecular field theory for the Frederiks transition has been developed based on the Lebwohl-Lasher nematogen model and localized mean field approximations. The comparison between theory and corresponding Monte Carlo simulation is also made. The agreement is fairly good considering the simplicity of the theory. Despite the simplicity of the theory, the director configurations, the cell thickness dependence of the threshold field, and the temperature dependence of the threshold obtained by Monte Carlo simulation are well reproduced by the present theory. We are quite optimistic that the Lebwohl-Lasher model can be extended to deal with more complicated systems such as nematic droplets with various director configurations and their field response. The system with unequal Frank's elastic constants, in principle, can also be treated with more realistic pair potentials. These topics will be dealt with in the future publications.

This work also lends support to the general validity of the Lebwohl-Lasher nematogen model for the treatment of small molecular thermotropic liquid crystals, which yields essentially exact results.

Acknowledgments

Financial support by National Basic Research Project–Macromolecular Condensed State, NSF of China and FEYUT, SEDC are gratefully acknowledged.

References

1. V. Frederiks, V. Zolina, *Zh. Russ. Fiz.-Khim. Ova., Chast. Fiz.*, **62**, 457 (1930); *Z. Kristallogr.* **79**, 255 (1931).
2. D. W. Berreman, *Philos. Trans. R. Soc., London*, **A309**, 203 (1983).

3. P. A. Breddels, H. A. van Sprang, *J. Appl. Phys.*, **58**, 2162 (1985).
4. M. E. Becker, B. B. Kosmowski, D. A. Mlynski, *Proc. SID*, **26**, 109 (1985).
5. I. Heynderickx, H. De Raedt, *Phys. Rev.* **A37**, 1725 (1988).
6. G. Lasher, *Phys. Rev.* **A5**, 1350 (1972).
7. P. A. Lebwohl, G. Lasher, *Phys. Rev.* **A6**, 426 (1972).
8. G. R. Luckhurst, P. Simpson, *Mol. Phys.*, **47**, 251 (1982).
9. C. Zannoni, M. Guerra, *Mol. Phys.*, **44**, 849 (1981).
10. C. Zannoni, *J. Chem. Phys.*, **84**, 424 (1986).
11. T. E. Faber, *Proc. R. Soc. A*, **370**, 509 (1980); **396**, 357 (1984).
12. G. R. Luckhurst, *The Molecular Physics of Liquid Crystals*, ed. by G. R. Luckhurst and G. W. Gray, Academic Press, Chapt., 4.
13. J. Lu, Y. Yang, *Sci. in China*, (*Ser. A*), **36**(5), 624 (1993).
14. P. G. de Gennes, *The Physics of Liquid Crystals*, Clarendon Press, 1974.
15. W. Maier, A. Saupe, *Z. Naturf.* **A13**, 564 (1958).
16. H. D. Zhang, J. Lu, Y. Yang, *Compt. Phys.* (Chinese), **9**, 2 (1992).
17. Y. Yang, J. Lu, H. D. Zhang, and T. Yu, *Polym. J.*, (accepted).
18. J. A. Baker, R. O. Watts, *Chem. Phys. Lett.*, **3**, 144 (1969).
19. E. S. Bedford, A. H. Windle, *Polym. Prep.*, **33**, 607 (1992).
20. V. Frederiks, V. Zolina, *Trans. Faraday Soc.*, **29**, 919 (1933).
21. H. Zocher, *Trans. Faraday Soc.*, **29**, 945 (1933).
22. A. Saupe, *Z. Naturf.* **A15**, 810 (1960).
23. H. Gruler, *Z. Naturf.* **A30**, 230 (1975).
24. H. J. Deuling, W. Welfrich, *Appl. Phys. Lett.*, **25**, 129 (1974).
25. H. L. Ong, *Phys. Rev.* **A28**, 2393 (1983); **A31**, 3450 (1985).
26. A. J. Karn, S. M. Arakelian, Y. R. Shen and H. L. Ong, *Phys. Rev. Lett.*, **57**, 448 (1986).
27. P. Wang, H. Zhang, J. Dai, *Opt. Lett.*, **12**, 654 (1987).
28. H. Deuling, *Mol. Cryst. Liq. Cryst.*, **19**, 123 (1972).
29. H. Gruler, T. J. Scheffer, G. Meier, *Z. Naturforsch*, **A27**, 966 (1972).